ELSEVIER

Powder Technology 94 (1997) 23–28

POWDER TECHNOLOGY

Fluidization of group B particles in an acoustic field

Lii-ping Leu *, Jiann-tzouh Li, Chia-Min Chen

Department of Chemical Engineering, National Taiwan University, Taipei 106-17, Taiwan

Received 8 November 1995; revised 21 April 1997; accepted 27 May 1997

Abstract

The behavior of group B particles (sand with mean diameter 194 μm) was studied in a sound wave vibrated fluidized bed (SVFB). The fluidized bed consists of a transparent Plexiglas tube of i.d. 54 mm and height 1 m. A loudspeaker mounted at the top of the bed was supplied by a function generator with square waves, and was used to generate the sound as the source of vibration of the fluidized bed. The effects of the power of the loudspeaker, sound frequencies, particle loading and the distance between the speaker and the bed surface on the hydrodynamic properties of the SVFB were investigated. The experimental results showed that the minimum fluidization velocity decreased with the addition of acoustic energy, and the standard deviation of pressure fluctuations became lower under the effect of sound. The sound wave also reduced the bubble rise velocity. The results were interpreted in terms of the operating parameters. © 1997 Elsevier Science S.A.

Keywords: Fluidization; Vibrated beds; Acoustic field; Sound waves

1. Introduction

Morse [1] was the first person to study the effect of sound on a fluidized bed. During his investigation, he put the loudspeaker at the bottom of the bed. He found that sufficient sonic energy (above 110 dB) of low frequency (from 50 to 500 Hz) will cause nonfluent group C particles [2] to flow sufficiently well that good fluidization is possible without channelling and stagnation. With group D particles [2], the effect is too small to be observed visually or to be detected with the capacitometer. Since then all research was limited to group C particles. Derczynski et al. [3] studied the effect of sonic energy on fluidization and heat transfer of fine particles which belong to group C powders. They found that the extent of bed expansion varies greatly according to the frequency of the sound; the highest increase in the heat transfer coefficient is at low frequencies, particularly at those at which resonance is secured. Nowak and Hasatani [4,5] have measured the fluidizability, the bulk density and relative heat transfer coefficient. They found that the addition of acoustic energy at low frequency significantly improves the quality of fluidization. They also found that the relative heat transfer coefficient increases with increase of sound energy. Chirone et al. [6] found that large clusters of group C powders are disaggregated into fluidizable subclusters by sound and such subclusters behave like a group A noncohesive material. They found bubble-free fluidization is obtained with an appropriate acoustic field when the large clusters originally present in beds fluidized without sound are broken into subclusters [7]. They also found that the break-up occurs at contact points where the external forces induced by the acoustic field are larger than the internal van der Waals forces. Leu and Huang [8] measured the interparticle forces of certain group C particles in fluidized beds by using sound waves to improve the quality of fluidization. Leu and Chen [9] put the speaker at the top of the bed to investigate the primary effect of acoustic sound on the fluidization of group B particles, and found that the minimum fluidization velocity decreases during the addition of sound waves.

In this study, the influence of sound on the minimum fluidization velocity, standard deviation of pressure fluctuations, bubble rise velocity and the hydrodynamic properties in group B particle fluidization systems was studied.

2. Experimental

The experimental apparatus is shown in Fig. 1. It consists of a fluidized column, a sound generation system and a data acquisition system. The fluidized column is constructed from a 54 mm i.d., 1 m high Plexiglas tube and has a perforated plate distributor. The perforated plate has 72 1.5 mm i.d. holes with a 5.8% open ratio. The distributor is covered with 200 mesh screen in order to prevent the solid particles flowing

* Corresponding author. Tel.: +886 2 365 7200; fax: +886 2 362 3040.

PII S0032-5910(97)03275-0

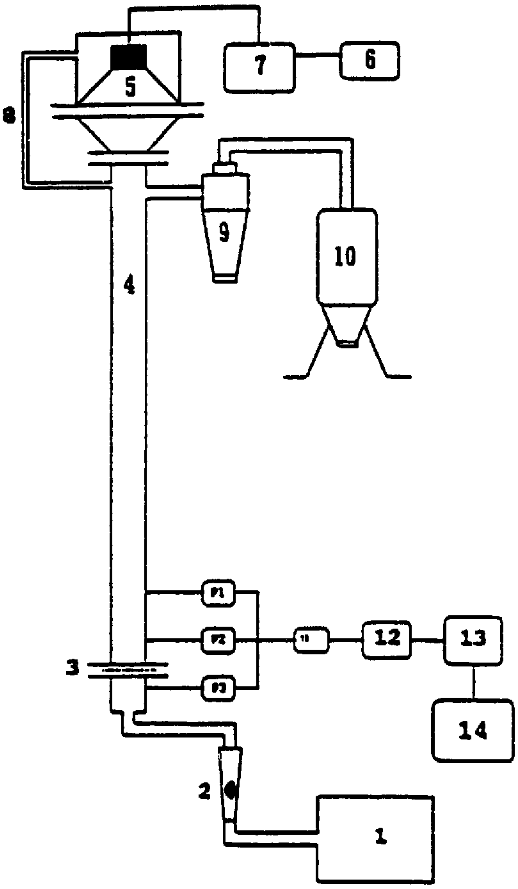

Fig. 1. Experimental setup: 1, Rootes blower; 2, gas rotameter; 3, distributor; 4, bed; 5, loudspeaker; 6, function generator; 7, high power amplifier; 8, pressure equilibrium line; 9, cyclone; 10, bag filter; 11, pressure transducer; 12, amplifier; 13, data acquisition system; 14, FFT analyzer; P1–P3, pressure taps.

into the holes. The bed is designed so that the bed length can be changed to adjust the distance between the bed surface and the speaker in order to get the resonance effect. Fluidization air was provided by a Rootes blower. A speaker rated at 30 W with an audible range frequency of 20 Hz–20 kHz located at the top of the bed was used to generate sound as the source of the acoustic field. It was powered with an audio amplifier, in turn supplied by a function generator. A balancing line was used to connect between the front and back sides of the speaker in order to equilibrate the pressure on both sides of the speaker. The pressure drops across the empty bed and the fluidized bed were measured by the pressure transducer and the signals were sent to a data acquisition system for future use. Group B sand particles (density 2635 kg/m^3) with size range 177–210 μm (mean size 194 μm) were used in all experiments. During the experiments, the effect of square waves was found to be stronger than that of other kinds of waves, so square waves were used in the subsequent analysis.

Here the following equation is used to define the degree of resonance (DOR):

$$\mathrm{DOR}=\sin\left[\frac{(2N+1)f}{f_r}\frac{\pi}{2}\right] \tag{1}$$

where f_r is the resonant frequency and f is the frequency used. The value of DOR is varied from zero to one; at $f=f_r$, $3f_r$, $5f_r$, ..., DOR = 1 (maximum value); at $f=0$, $2f_r$, $4f_r$, ..., DOR = 0 (minimum value). The DOR value represents the degree of deviation of the frequency used from the resonant frequency.

3. Results and discussion

3.1. Minimum fluidization velocity

When sound waves were applied to the particulate bed, the particles in the bed tended to be in a denser condition, so the hysteresis state [10] in the pressure drop versus superficial velocity curve could not occur. The minimum fluidization velocity was then determined from the gas velocity at which the maximum pressure drop point in the pressure drop versus superficial gas velocity curve was first reached.

The effect of sound waves on the minimum fluidization velocity is shown in Fig. 2. The minimum fluidization velocity decreased as the sound energy increased and approached a constant value if the sound energy was strong enough. The bed pressure drop was nearly the same as that without sound [11]. This result is different from that obtained by Nowak et al. [5] for group C particles: they found a lower pressure drop in the presence of sound. Nowak et al. showed theoretically that the minimum fluidization velocity may be expected to decrease in the presence of sound of sufficient energy. The result shown in Fig. 2 is as expected from their analysis. It can be seen that the minimum fluidization velocity decreased as the output power of the speaker increased for a given frequency. Also, it was found that for $f=f_r=100$ Hz, DOR = 1, the effect on the minimum fluidization velocity was greater than with sound of other frequencies. The mini-

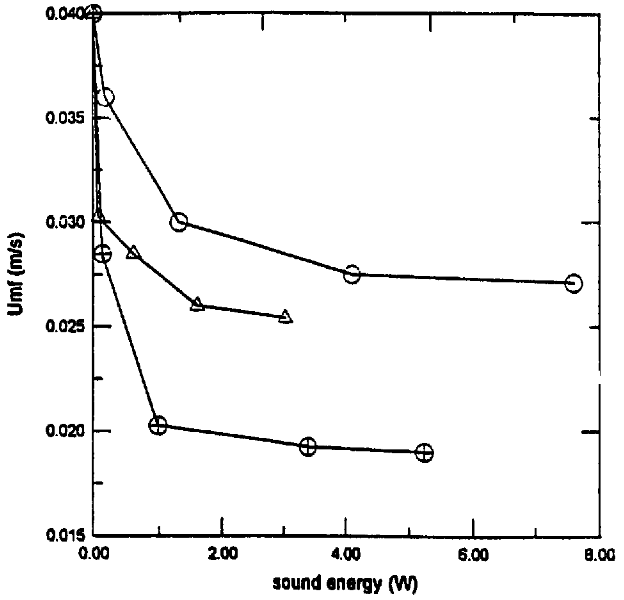

Fig. 2. Effect of sound energy on U_{mf} in the acoustic field (W_p=0.39 kg, f_r=100 Hz): –○–, 130 Hz, DOR=0.891; –△–, 70 Hz, DOR=0.891; –⊕–, 100 Hz, DOR=1.

mum fluidization velocity approached a constant-value minimum fluidization velocity $U_{mf\infty}$ at a certain power input. After that, an increase of power had no effect on the minimum fluidization velocity; this value of power was termed the critical power. The critical power P_c is defined empirically here as

$$P_c = KW_p g L_s / A \quad (2)$$

where W_p and L_s represent the bed particle loading and the distance which the sound wave must travel (the distance from the sound source to the surface of the bed), respectively, and K is an experimental constant with a value of about 3×10^{-3} m^2/s here. P_c is a function of the bed height (bed particle loading), bed area, distance the sound wave must travel and the kind of fluid medium for transmission. If the power used were less than the critical power, the minimum fluidization velocity would decrease as the power increased and approach a constant value $U_{mf\infty}$. As the power exceeded the critical power the minimum fluidization velocity became independent of power and only depended on the frequency (or DOR value) used.

3.2. *Effect of bed particle loading (or static bed height) on the minimum fluidization velocity*

In an ordinary fluidized bed, the minimum fluidization velocity is constant and independent of the static bed height or bed particle loading, but in the SVFB the result is quite different: the bed particle loading changes the static bed height, and the resonant frequency can be changed.

The effect of bed particle loading on the minimum fluidization velocity at a frequency of sound of 70 Hz is shown in Fig. 3. Thus, for $W_p = 0.298$ kg, the sound with DOR = 0.987 was close to the resonant condition and the minimum fluidization velocity was lowest. After addition of particles, the length of the empty tube was changed, and the resonant frequency also changed. The DOR then became 0.891, and the change in minimum fluidization velocity was smaller. The minimum fluidization velocity would approach the same value despite the bed particle loading if the frequency were adjusted to have the same DOR value. This is shown in Fig. 4 where, for different bed particle loadings, the frequency used was adjusted to obtain the same DOR value, providing sufficient power is applied. When the bed particle loading was kept constant, but different DOR values were used (by using different lengths of empty tube above the bed surface), different minimum fluidization velocities were obtained (Fig. 5). The effect was inversely proportional to the DOR value. However, Fig. 2 shows that different minimum fluidization velocities were obtained for the same DOR value, which would seem to be contrary to the above conclusion that the same DOR value gives the same minimum fluidization velocity, i.e. the same minimum fluidization velocity would be obtained for the long length of empty tube if the power exceeded the critical power P_c. This is because the distance for sound transmission for different loadings would change with the change in empty tube length, so changing the value of the critical power but not the minimum fluidization velocity. In other words, if the power and the frequency of the sound were adjusted, the minimum fluidization velocity would then remain constant regardless of the bed particle loading despite the change in bed length.

3.3. *Pressure drop in a sound wave vibrated fixed bed*

The pressure drop in a sound wave fixed bed was calculated from the Ergun equation. Without sound the following equa-

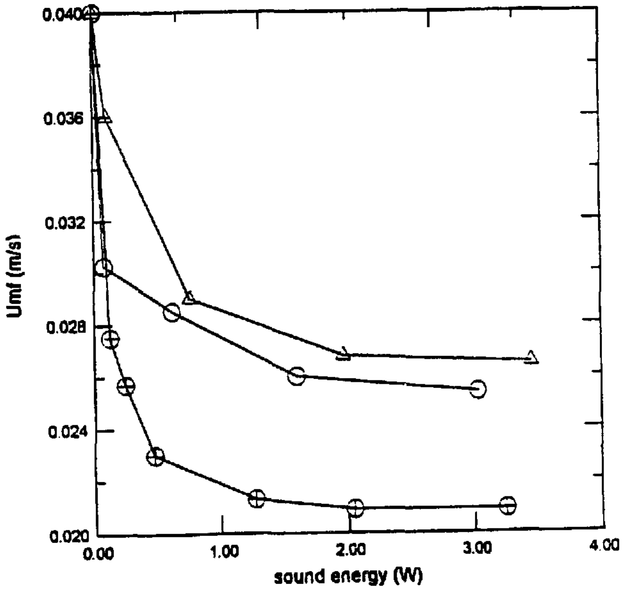

Fig. 3. Effect of sound energy, W_p and DOR on U_{mf}: –△–, $W_p = 0.596$ kg, 70 Hz, DOR = 0.851; –○–, $W_p = 0.39$ kg, 70 Hz, DOR = 0.891; –⊕–, $W_p = 0.298$ kg, 70 Hz, DOR = 0.987.

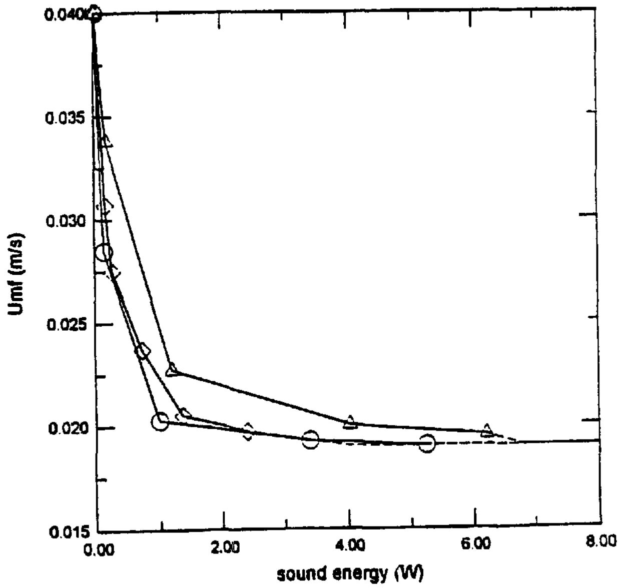

Fig. 4. The effect of sound energy, W_p and DOR on U_{mf}: –△–, $W_p = 0.596$ kg, 108 Hz, DOR = 1; –◇–, $W_p = 0.298$ kg, 78 Hz, DOR = 1; –○–, $W_p = 0.393$ kg, 100 Hz, DOR = 1.

j41

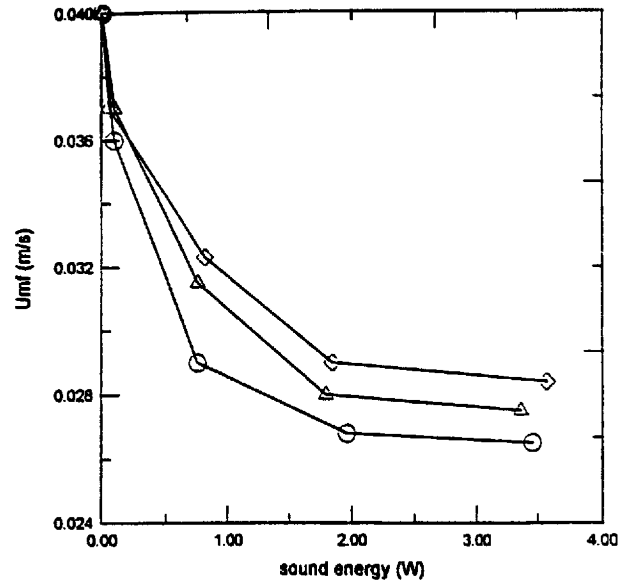

Fig. 5. Effect of sound energy, L_s and DOR on U_{mf} at $W_p = 0.596$ kg, $f = 70$ Hz: –◇–, $L_s = 0.83$ m, DOR = 0.851; –△–, $L_s = 0.9$ m, DOR = 0.891; –○–, $L_s = 1.053$ m, DOR = 0.962.

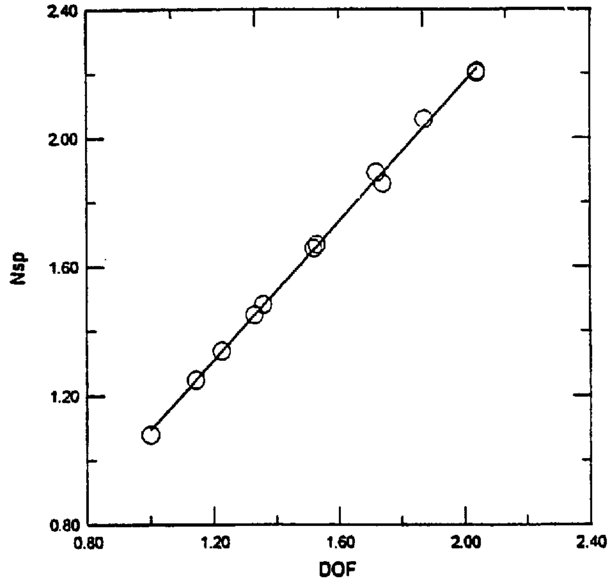

Fig. 6. N_{sp} vs. DOF of sound wave vibrated fluidized bed: ○, N_{sp} vs. DOF; ———, linear, $Y = BX + A$, slope = 1.08.

tion was obtained for a fixed bed at the minimum fluidization condition:

$$\Delta P_{mf0}/L_{bmf0} \approx a_{mf0}U_{mf0} \quad Re_p < 1 \tag{3}$$

and for a sound wave fixed bed at the minimum fluidization condition:

$$\Delta P_{mfs}/L_{bmfs} \approx a_{mfs}U_{mf} \quad Re_p < 1 \tag{4}$$

Eq. (3) was divided by Eq. (4) and rearranged to give

$$L_{bmfs}a_{mfs}/L_{bmf0}a_{mf0} = \Delta P_{mfs}U_{mf0}/\Delta P_{mf0}U_{mf} \approx CU_{mf0}/U_{mf} \tag{5}$$

We define

$$N_{sp} = \text{sound pressure number} = L_{bmfs}a_{mfs}/L_{bmf0}a_{mf0} \tag{6}$$

$$\text{DOF} = \text{degree of fluidization} = U_{mf0}/U_{mf} \tag{7}$$

From experimental data and various DOR values, N_{sp} and DOF can be calculated. The relationship between N_{sp} and DOF is shown in Fig. 6.

The procedure for calculating the pressure drop in the sound wave vibrated fixed bed is as follows:

For given values of a_{mf0}, ΔP_{mf0}, U_{mf0} and L_{bmf0}:

1. Find the critical power P_c from Eq. (2).
2. From the length of the empty tube, calculate the resonant frequency by $f_r = (2N+1)V/4L_s$.
3. Find DOR by Eq. (1).
4. From Fig. 7 find U_{mf} and calculate DOF by Eq. (7).
5. From Fig. 6 find N_{sp} and get a_{mfs}.
6. Calculate $\Delta P_s/L_{bs}$ in the sound wave vibrated fixed bed by using the equation

$$\Delta P_s/L_{bs} \approx a_{mfs}U \tag{8}$$

A similar method could be used to calculate the frequency used and the critical power if the pressure drop were known.

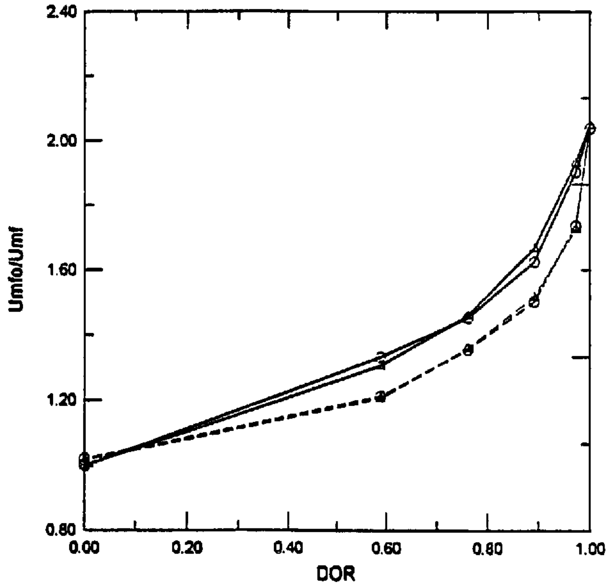

Fig. 7. Effect of DOR on U_{mf0}/U_{mf} at P_c: –○–, $W_p = 0.39$ kg, 0–f_r; --○--, $W_p = 0.39$ kg, f_r–2f_r; –△–, $W_p = 0.596$ kg, 0–f_r; --△--, $W_p = 0.596$ kg, f_r–2f_r.

3.4. Standard deviation of pressure fluctuations

Fig. 8 shows the standard deviation of pressure fluctuations versus excess velocity. At fixed values of the excess velocity, $U - U_{mf}$, the standard deviation of the pressure fluctuations decreased compared with the corresponding one without the sound effect. This means that the sound has the effect of reducing the pressure fluctuations, i.e. the fluidized bed has a better quality in the acoustic field. This result was contrary to the results obtained by Morse [1] who found no improvement in the quality of fluidization with sonic energy for free-flowing particles. The standard deviation of the pressure fluc-

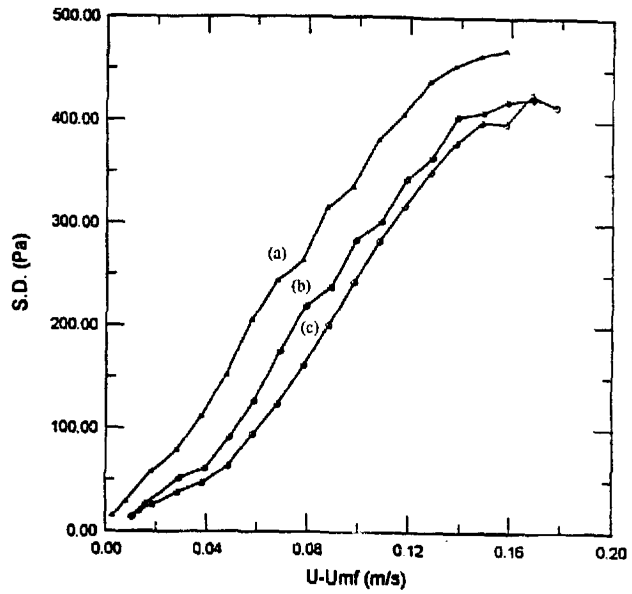

Fig. 8. Effect of $U-U_{mf}$ on the standard deviation of pressure fluctuations at different conditions: – △ – (curve a) without sound; – ⊕ – (curve b), 70 Hz, DOR = 0.851, 3.5 W; – ○ – (curve c), 108 Hz, DOR = 1.5 W.

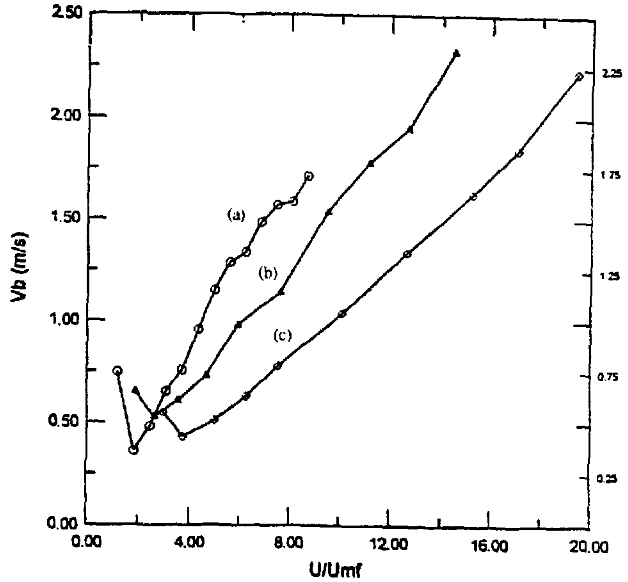

Fig. 10. Effect of U/U_{mf} on the mean bubble rise velocity at different conditions: – ○ – (curve a), without sound; – △ – (curve b), DOR = 0.891, 3.6 W; – ◇ – (curve c), DOR = 1.5 W.

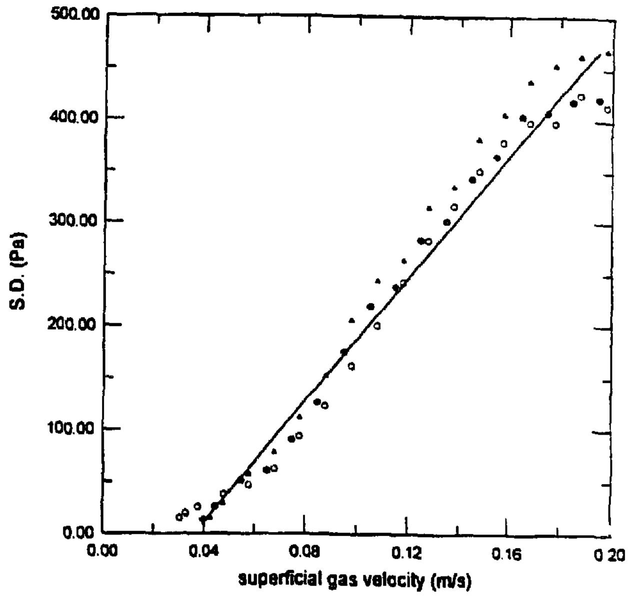

Fig. 9. Effect of superficial gas velocity on the standard deviation of pressure fluctuations at different conditions: △, without sound; ○, 108 Hz, DOR = 1.5 W; ⊕, 70 Hz, DOR = 0.851, 3.5 W.

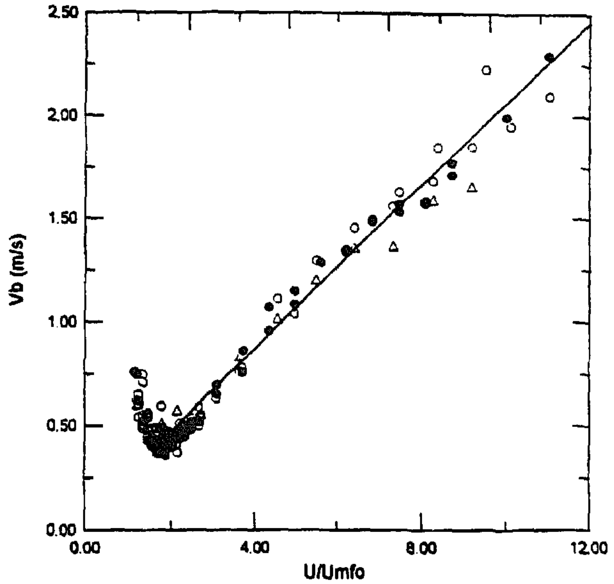

Fig. 11. Effect of U/U_{mfo} on the mean bubble rise velocity at different conditions: ○, DOR = 1.5 W; △, DOR = 0.891, 3.6 W; ●, without sound.

tuations was plotted against the superficial gas velocity and a straight line was obtained (Fig. 9). No matter what the value of DOR was for the system, with or without the sound effect, the standard deviation of the pressure fluctuations across the bed was the same at the same superficial gas velocity.

3.5. Bubble rise velocity

The bubble rise velocity was measured by taking the cross-correlation function between two pressure fluctuation signals and was calculated following Sitnai [12]. Thus, the bubble rise velocity can be obtained as

$$V_b = L/\tau_p$$

where L is the distance between the two pressure probes and τ_p is the time lag in the cross-correlation of the pressure fluctuation signals. Each time the lag data were averaged over 50 time lag data sets and each data set was calculated from 8192 pressure fluctuation signal points. The bubble rise velocity obtained is shown in Fig. 10. The sound had the effect of reducing the bubble rise velocity. All the data for bubble rise velocity versus U/U_{mf} could be correlated well by a single straight line except in the low velocity range (Fig. 11).

4. Conclusions

The hydrodynamic behavior of group B particles was studied in a sound wave vibrated fluidized bed. The sound reduces the minimum fluidization velocity. The main parameters involved in this effect are the degree of resonance (DOR) and the power of the sound. If the power is high enough (higher than the critical power), then the same DOR will give the same minimum fluidization velocity. The DOR corresponding to the resonant effect has the strongest effect on the minimum fluidization velocity. The bed particle loading or static bed height influences the DOR value. The sound also reduces the standard deviation of the pressure fluctuations and the bubble rise velocity, the effect being correlated well by a simple straight line.

5. List of symbols

a_{mf0}	constant defined by Eq. (3)
a_{mfs}	constant defined by Eq. (4)
C	constant
DOF	degree of fluidization
DOR	degree of resonance
f	frequency of sound used (Hz)
f_r	resonant frequency (Hz)
g	acceleration due to gravity (m/s^2)
L	distance between pressure probes (m)
L_{bmf0}	bed height at minimum fluidization without sound effect (m)
L_{bmfs}	bed height at minimum fluidization with sound effect (m)
L_{bs}	bed height with sound effect (m)
L_s	empty tube length (m)
N	integer
N_{sp}	sound pressure number
P_c	critical power defined by Eq. (2) (W)
ΔP_{mf0}	pressure drop at minimum fluidization condition without sound effect (Pa)
ΔP_{mfs}	pressure drop at minimum fluidization condition with sound effect (Pa)
ΔP_s	pressure drop across bed with sound effect (Pa)
Re_p	particle Reynolds number
S.D.	standard deviation of pressure fluctuations (Pa)
U	superficial gas velocity (m/s)
U_{mf}	minimum fluidization velocity (m/s)
U_{mf0}	minimum fluidization velocity without sound effect (m/s)
$U_{mf\infty}$	minimum fluidization velocity limit (m/s)
V	velocity of sound wave (m/s)
V_b	bubble rise velocity (m/s)
W_p	bed particle loading (kg)

Greek letters

τ_p	time lag in cross-correlation of pressure fluctuation signals (s)

Acknowledgements

The authors are grateful to the National Science Council, R.O.C., for financial support.

References

[1] R.D. Morse, Ind. Eng. Chem., 47 (1955) 1170.
[2] D. Geldart, Powder Technol., 7 (1973) 285.
[3] M. Derczynski, Z. Bis, W. Gajewski and W. Nowak, 4th World Congr. Chemical Engineering, Karlsruhe, Germany, 1991, Paper 9.5-37.
[4] W. Nowak and M. Hasatani, in H.S. Chun and S.D. Kim (eds.), Proc. 3rd Asian Conf. Fluidized-Bed and Three-Phase Reactors, Kyongju, South Korea, 1992, p. 423.
[5] W. Nowak, M. Hasatani and M. Derczynski, AIChE Symp. Ser., 89 (1993) 137.
[6] R. Chirone, L. Massimilla and S. Russo, Chem. Eng. Sci., 48 (1993) 41.
[7] R. Chirone, L. Massimilla and S. Russo, in O E. Potter and D.J. Nicklin (eds.), Fluidization VII, Engineering Foundation, New York, 1992, p. 545.
[8] L.P. Leu and C.T. Huang, AIChE Symp. Ser., 90 (1994) 301.
[9] L.P. Leu and C.M. Chen, in K. Yoshida and S. Morooka (eds.), Proc. Asian Conf. Fluidized-Bed and Three-Phase Reactors, Fukuoka, Japan, 1994, p. 13.
[10] J.F. Davidson and D. Harrison, Fluidised Particles, Cambridge University Press, New York, 1963, p. 4.
[11] J.T. Li, Master Thesis, Department of Chemical Engineering, National Taiwan University, 1995.
[12] O. Sitnai, Chem. Eng. Sci., 37 (1982) 1059.